

# Topological structure analysis of the protein–protein interaction network in budding yeast

Dongbo Bu<sup>1</sup>, Yi Zhao<sup>1</sup>, Lun Cai<sup>1</sup>, Hong Xue<sup>2</sup>, Xiaopeng Zhu<sup>2</sup>, Hongchao Lu<sup>1</sup>,  
Jingfen Zhang<sup>1</sup>, Shiwei Sun<sup>1</sup>, Lunjiang Ling<sup>2</sup>, Nan Zhang<sup>2</sup>, Guojie Li<sup>1</sup> and  
Runsheng Chen<sup>1,2,\*</sup>

<sup>1</sup>Bioinformatics Research Group, Key Laboratory of Intelligent Information Processing, Institute of Computing Technology and <sup>2</sup>Bioinformatics Laboratory, Institute of Biophysics, Chinese Academy of Sciences, Beijing, China

Received October 15, 2002; Revised January 13, 2003; Accepted March 3, 2003

## ABSTRACT

Interaction detection methods have led to the discovery of thousands of interactions between proteins, and discerning relevance within large-scale data sets is important to present-day biology. Here, a spectral method derived from graph theory was introduced to uncover hidden topological structures (i.e. quasi-cliques and quasi-bipartites) of complicated protein–protein interaction networks. Our analyses suggest that these hidden topological structures consist of biologically relevant functional groups. This result motivates a new method to predict the function of uncharacterized proteins based on the classification of known proteins within topological structures. Using this spectral analysis method, 48 quasi-cliques and six quasi-bipartites were isolated from a network involving 11 855 interactions among 2617 proteins in budding yeast, and 76 uncharacterized proteins were assigned functions.

## INTRODUCTION

With the availability of complete DNA sequence data for many prokaryotic and eukaryotic genomes, a formidable challenge of post-genomic biology is to understand how genetic information results in the concerted action of gene products both temporally and spatially to achieve biological function, as well as how they interact with each other to create an organism. It is important to develop reliable proteome-wide approaches for a better understanding of protein functions (1,2). Genomic approaches have been used to predict functions of a large number of genes based on their sequences. However, as we know, proteins rarely act alone at the biochemical level; rather, they interact with other proteins as an assembly to perform particular cellular tasks. Having systematic functions, these assemblies represent more than the

sum of their parts (3). Traditionally, protein interactions were studied individually by genetic, biochemical and biophysical techniques focusing on a few proteins at a time (4). It is increasingly realized that dissecting the genetic and biochemical circuitry of a cell prevents us from further understanding the biological processes as a whole. Basic constituents of cellular protein complexes and pathways, protein–protein interactions are key determinants of protein function. It is believed that all biological processes are essentially and accurately carried out through protein–protein interactions.

In the last 3 years, high-throughput interaction detection approaches, such as yeast two-hybrid systems (5,6), protein complex purification techniques using mass spectrometry (3,7), correlated messenger RNA expression profiles (8,9), genetic interaction data (10,11) and ‘*in silico*’ interaction predictions derived from gene context analysis [gene fusion (12,13), gene neighborhood (14,15) and gene co-occurrences or phylogenetic profiles (16,17)], have been developed and they have created a number of datasets regarding protein–protein interactions for several model organisms (*Saccharomyces cerevisiae*, *Caenorhabditis elegans* and *Helicobacter pylori*). These large-scale datasets open a door to comprehensive understanding of the genetic and biochemical phenomena in a cell. Subsequently, several promising methods have been successfully applied to this field. For instance, Schwikowski *et al.* (18) and Hishigaki *et al.* (19) predicted uncharacterized proteins based on interacting partners; Maslov and Sneppen (20) analyzed the stable topological properties of interaction networks; Ge *et al.* (21) provided the first global evidence that genes with similar expression profiles are more likely to encode interacting proteins; and Fraser *et al.* (22) revealed that the connectivity of well-conserved proteins in the network is negatively correlated with their rate of evolution. These studies revealed that the available data from protein–protein interaction networks in *S.cerevisiae* share some unexpected features with other complex networks.

The topological pattern of interactions is a rich source of biological functional information, and therefore we need to

\*To whom correspondence should be addressed at Bioinformatics Laboratory, Institute of Biophysics, Chinese Academy of Sciences, Beijing, China.  
Tel: +8610 64888543; Fax: +8610 64871293; Email: crs@sun5.ibp.ac.cn  
Correspondence may also be addressed to Guojie Li. Tel: +8610 62565533; Fax: +8610 62567724; Email: lig@ict.ac.cn

The authors wish it to be known that, in their opinion, the first two authors should be regarded as joint First Authors

develop methods to mine and to understand the interaction networks. Here, we applied the spectral analysis method, which has been successful used in other fields (23), to proteomics to identify topological structures of interaction networks, i.e. quasi-cliques and quasi-bipartites. Interestingly, we found that the proteins within same group share similar biological functions. Moreover, for one-third of proteins that are still uncharacterized in *S.cerevisiae*, this method provides a new approach to predict their functions based on topological structures.

## MATERIALS AND METHODS

### Spectral analysis

Spectral analysis is a powerful tool to reveal high-level structures underlying enormous and complicated relationships. As a famous paradigm, David Gibson, Jon Kleinberg and Prabhakar Raghavan did excellent work on extracting information from link structure of the Web (23,24). The World Wide Web is known to be composed of an increasing number of pages with hyperlinks pointing to other pages. Despite high complexity of the Web structure, spectral analysis was successfully used to discover 'authoritative' information sources and 'hub' pages joining authoritative ones together.

We applied the spectral analysis method to complicated protein-protein interaction networks and identified interesting topological structures. In this method, a network is represented by a bi-directed graph  $G(V,E)$ , i.e. vertex set including each protein as a vertex  $V = \{P_1, P_2, \dots, P_n\}$ , and the edge set  $E = \{(P_i, P_j) | \text{there is an interaction between protein } P_i \text{ and } P_j\}$ . The symmetric  $n \times n$  adjacent matrix is defined as  $A = (a_{ij})$ , where  $a_{ij} = 1$  if  $(P_i, P_j) \in E$ , and  $a_{ij} = 0$  if  $(P_i, P_j) \notin E$ .

Spectrum of the adjacency matrix  $A$  is essentially a reasonable measurement of properties of nodes that could be propagated across the interactions. Let us consider assigning a score to each node to represent their intensity, say  $X$ . A node with a high score would increase its neighbors' score through their interactions. In other words, two nodes are mutually reinforcing, which is in nature a cyclic definition of scores:

$$\Delta X_i = \sum_{j=1}^n a_{ij} \times X_j$$

The iteration method derived from Gibson *et al.* (23) and Kleinberg (24) is introduced to break such a cycle. It is interesting that  $X_i$  converges to a fixed point from any initializing assignment, and it can be proved that the fixed point is one of the eigenvectors of matrix  $A$ , which means it is an intrinsic characteristic of interactions. Moreover, since matrix  $A$  is symmetric, all of its eigenvectors are mutually orthogonal, which means that the corresponding properties are also mutually independent. In other words, each eigenvector represents a special property that none of the others could represent.

### Identification of topological structures

From a topological point of view, the spectrum helps to uncover the hidden topological structures of a complex interaction network. We found that for each eigenvector with a positive eigenvalue, the proteins corresponding to absolutely larger components tend to form a quasi-clique

(i.e. every two of them tend to interact with each other) (Fig. 1a), whereas for each eigenvector with a negative eigenvalue, such proteins tend to form a quasi-bipartite (i.e. the proteins in which two disjoint subsets express high level connectivity between sets rather than within sets) (Fig. 1b).

This observation can be explained as follows. The maximal eigenvalue of an adjacent matrix is the maximal value of

$$Q(\vec{x}) = \sum_{i=1}^m A_{ij} x_i x_j = \sum_{v_i, v_j \in E} x_i x_j \text{ subjected to } \sum_{i=1}^m x_i x_i = 1$$

(where  $x_i$  is the  $i$ th component of the eigenvector). Other positive eigenvalues can also be described as the maximal value  $Q$  with orthogonal condition. Since  $Q$  is the summary of  $x_i x_j$  corresponding to edge  $v_i v_j$ , it would be maximal when the nodes with more edges are assigned a larger value with the same signal, which form a quasi-clique intuitively. Similar quasi-bipartites would be obtained eigenvectors with negative eigenvalues.

We applied the clustering coefficient (CC) (25,26) in our analysis to quantify a quasi-clique's tendency to form a cluster. The ratio between the number of edges that actually exist between these  $N$  nodes and the total number  $N(N-1)/2$  gives the CC-value of a quasi-clique, i.e.  $CC = E/[N*(N-1)/2]*100\%$ , where  $E$  is the number of interactions within the clique and  $N$  is the number of proteins in it. CC is greater than 0 and less than 1. A value close to 1 represents a clique close to a complete graph.

### Assignment of annotation and $P$ -values to quasi-cliques

As an isolated quasi-clique may involve different functional categories,  $P$ -values (27,28) are used as criteria to assign each quasi-clique a main function. Hypergeometric distribution was applied to model the probability of observing at least  $k$  proteins from a quasi-clique size  $n$  by chance in a category containing  $C$  proteins from a total genome size of  $G$  proteins, such that the  $P$ -value is given by

$$P = 1 - \sum_{i=0}^{k-1} \frac{\binom{C}{i} \binom{G-C}{n-i}}{\binom{G}{n}}$$

The above test measures whether a quasi-clique is enriched with proteins from a particular category more than would be expected by chance. If the  $P$ -value of a category is near 0, the proteins of the category in a quasi-clique will have a low probability of being chosen by chance. Here, we assigned each quasi-clique the main function with the lowest  $P$ -value in all categories.

## RESULTS

### Data source and analysis

Among the interactions produced by high-throughput methods there could be many false positives. To measure their accuracy and to identify the biases, von Mering *et al.* (4) assessed a total of 80 000 interactions among 5400 yeast proteins reported previously and assigned each interaction a confidence value. In order to reduce the interference by false positives, we focused on 11 855 interactions with high and medium confidence among 2617 proteins.

**Table 1.** Annotation of all quasi-cliques

No.	Protein no.	Interaction no.	CC (%)	Distribution (%)			P-value (log <sub>10</sub> )	Function
				M	U	D		
1	109	2978	50	72	6	22	75	Ribosome biogenesis
2	97	2327	49	72	5	23	67	Ribosome biogenesis
3	68	955	41	19	50	31	10	rRNA processing
4	44	570	60	18	50	32	6	rRNA processing
5	37	423	63	19	49	32	6	rRNA processing
6	34	239	42	76	15	9	25	Ribosome biogenesis
7	24	230	83	50	0	50	15	General transcription activities
8	40	333	42	80	10	10	47	Splicing
9	34	329	58	9	50	41	5	Other tRNA-transcription activities
10	54	1018	71	78	9	13	41	Ribosome biogenesis
11	24	200	72	79	4	17	28	Cytoplasmic and nuclear degradation
12	44	410	43	59	11	30	20	Ribosome biogenesis
13	32	267	53	34	3	63	15	rRNA synthesis
14	34	214	38	18	21	61	7	Amino acid degradation (catabolism)
15	21	153	72	52	14	34	14	rRNA processing
16	31	189	40	39	19	42	7	Oxidation of fatty acids; lipid, fatty-acid and isoprenoid biosynthesis
17	27	251	71	11	67	22	2	tRNA transcription; other control of cellular organization; other transcription activities
18	16	106	88	63	19	18	16	mRNA processing (splicing, 5'-, 3'-end processing)
19	21	119	56	57	24	19	9	Ribosome biogenesis
20	35	281	47	60	3	37	17	Ribosome biogenesis
21	24	119	43	25	21	54	5	Lipid, fatty-acid and isoprenoid biosynthesis
22	16	62	51	19	13	68	7	Osmosensing; protein binding
23	13	78	100	69	31	0	8	Ribosome biogenesis
24	27	157	44	56	4	40	25	rRNA synthesis
25	14	46	50	36	7	57	6	Respiration
26	28	142	37	50	0	50	23	rRNA synthesis
27	21	134	63	71	0	29	20	Splicing
28	23	153	60	65	17	18	19	Splicing
29	17	86	63	82	0	18	27	rRNA synthesis
30	18	92	60	89	0	11	32	Transport ATPases
31	19	84	49	37	5	58	11	Tricarboxylic-acid pathway (citrate cycle, Krebs cycle, TCA cycle)
32	15	70	66	40	7	53	6	Lipid, fatty-acid and isoprenoid biosynthesis
33	11	51	92	27	9	64	4	Homeostasis of metal ions (Na, K, Ca, etc.)
34	12	57	86	33	8	59	6	Homeostasis of metal ions (Na, K, Ca, etc.)
35	20	96	50	35	5	60	11	Tricarboxylic-acid pathway (citrate cycle, Krebs cycle, TCA cycle)
36	11	45	82	55	27	18	2	Assembly of protein complexes; lipid, fatty-acid and isoprenoid biosynthesis; cell wall
37	11	51	93	27	9	64	4	Homeostasis of metal ions (Na, K, Ca, etc.)
38	19	136	79	79	5	16	22	Cytoplasmic and nuclear degradation
39	13	72	92	100	0	0	22	Cytoplasmic and nuclear degradation
40	14	59	64	29	21	50	2	Aminoacyl-tRNA-synthetases; cell wall
41	13	47	60	54	8	38	12	Tricarboxylic-acid pathway (citrate cycle, Krebs cycle, TCA cycle)
42	12	58	88	42	8	50	5	Lipid, fatty-acid and isoprenoid biosynthesis
43	19	91	53	21	37	42	4	rRNA processing
44	11	52	94	64	9	27	6	Ribosome biogenesis
45	10	24	53	50	0	50	5	Amino acid biosynthesis
46	11	52	94	64	9	27	6	Ribosome biogenesis
47	15	40	38	20	0	80	6	Other proteolytic degradation
48	15	51	48	40	20	40	6	Lipid, fatty-acid and isoprenoid biosynthesis

No., quasi-clique no. Protein no., the number of proteins in the quasi-clique. Interaction no., the number of interactions within the quasi-clique. CC, represents the CC-value of a quasi-clique (see Materials and Methods). Function, the assigned function of the quasi-clique. Distribution, percentages of the following three classes in the quasi-clique: M, the percentage of proteins which have the main function; U, the percentage of uncharacterized proteins and D, the percentage of proteins which are discordant with the quasi-clique's function.

To analyze the interaction dataset, first we applied the spectral method to calculate all eigenvalues and eigenvectors of the adjacency matrix corresponding to the network. The following criteria were then used to generate quasi-cliques based on eigenvectors with larger and positive eigenvalues. (i) All the proteins were sorted by their absolute weight value in an eigenvector, and the top 10% were selected. (ii) Every protein must interact with at least 20% of the members. Here, we used CC-value to measure the degree of the interconnectivity between nodes and tuned the parameter to guarantee the quality of those cliques. (iii) A quasi-clique must contain at

least 10 proteins. As a result, we yielded 48 quasi-cliques, among which the largest one contains 109 proteins (quasi-clique 1 in Table 1) and the smallest one contains 10 proteins (quasi-clique 45 in Table 1); on average, a quasi-clique contains 26.6 proteins (a protein may appear in different quasi-cliques). Similar analysis based on eigenvector with negative eigenvalue produced six quasi-bipartites.

The two topological structures show different interaction patterns. In a quasi-clique proteins tend to interact with each other (Fig. 1a), while in a quasi-bipartite, proteins between sets have denser interactions than those within sets (Fig. 1b).

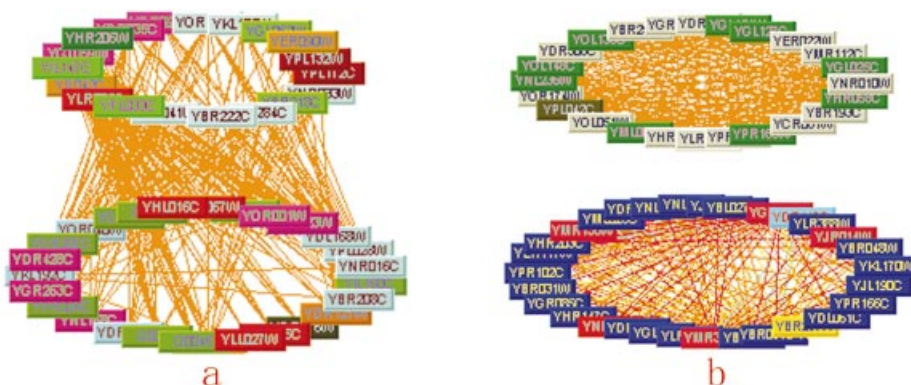


**Figure 1.** The topological structures of protein-protein interaction networks. In a quasi-clique, proteins tend to interact with each other (a), while in a quasi-bipartite, proteins between sets have denser interactions than those within sets (b).

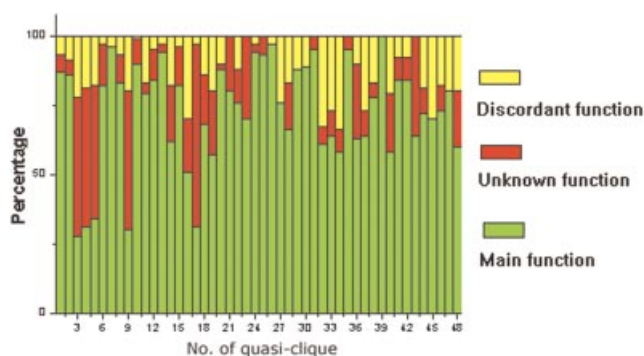


**Figure 2.** The percentage of functional classes of the 48 quasi-cliques. Distribution of the following three classes: main function, percentage of the proteins that have the main function; unknown function, percentage of the uncharacterized proteins; and discordant function, percentage of the proteins that have discordant functions.

Identification of the above topological structures could not only represent the complicated interaction network in order, but also make the complicated network more convenient to analyze.

### Annotation of quasi-cliques

For each of the 48 quasi-cliques, we calculated its  $P$ -value and annotated it based on the Munich Information Center (MIPS) hierarchical functional categories. MIPS allows a protein to appear in more than one category, which was taken into account in the calculation of  $P$ -value. As a result, 43 quasi-cliques were annotated with one functional category and the other five quasi-cliques were assigned to a set of functional categories (Table 1; see Supplementary Material for complete data sets).

We investigated the functions of individual proteins in quasi-cliques and found that most of them usually share common functions, including ribosome biogenesis, rRNA and tRNA synthesis, processing, transcription control and mRNA splicing, etc. (Fig. 2 and Table 1). Only a small fraction of the proteins turn out uncharacterized or have functions conflicting with the common function of the quasi-clique, as shown in Figure 2. This could be explained by either unavoidable false positive interactions under the current experimental

conditions or that the proteins really share this kind of function but it is yet not proved.

To visualize protein interactions and functional annotations, we have developed a software package that, along with the complete set of data generated by our algorithm, is publicly available at <http://www.bioinfo.org.cn/PIN/>. Using this software, users can view topological structures and find annotations of proteins and their interactions conveniently.

### Functional prediction for uncharacterized proteins in quasi-cliques

The isolated quasi-cliques give a good clue to predict functions of the uncharacterized proteins. Among the 2617 proteins in the raw dataset, 555 were uncharacterized according to MIPS hierarchical functional categories (4). For the 76 uncharacterized proteins in the 48 quasi-cliques, we assigned for each one a function according to the main function of its hosting quasi-clique. If a protein falls into more than one quasi-clique, the main function of the quasi-clique with the lowest  $P$ -value was assigned to it. If multiple hosting quasi-cliques have the lowest  $P$ -value, or a quasi-clique has multiple main functions, a set of functions would be assigned to the protein. The 76 unknown proteins and their predicted functions with the corresponding  $P$ -values are listed in Table 2. There are 43 rRNA processing proteins, seven proteins related to pre-rRNA processing, 11 proteins related to ribosome biogenesis, and the other 15 proteins related to energy, metabolism, cytoskeleton and transcription-regulating (See Table 2 for complete data).

We assessed the ability of the  $P$ -value to annotate and assign functions using the same approach as Wu *et al.* (28). As a control, we created and analyzed random networks with the same interaction distribution as the original network. The results show that among the 48 quasi-cliques of our experimental data, >87.5% were significant in one or more annotation categories at  $P \leq 0.01/N_c$  (here  $N_c$  is the number of categories), whereas <2.1% of quasi-cliques identified from random network met the same criteria. This means a substantial fraction of isolated quasi-cliques are likely to be biologically meaningful.

Some of our predictions were supported by recent experimental evidence. Of all the quasi-cliques, five were dominated by uncharacterized proteins (functions are unknown for at

**Table 2.** Prediction for uncharacterized proteins involved in 48 quasi-cliques

Protein	P-value (log <sub>10</sub> )	Predicted function
YLR421C	28	Cytoplasmic and nuclear degradation
YNL168C	7	Amino acid degradation (catabolism)
YDL193W	6	Lipid, fatty-acid and isoprenoid biosynthesis
YDR018C	6	Lipid, fatty-acid and isoprenoid biosynthesis
YNL026W	6	Lipid, fatty-acid and isoprenoid biosynthesis
YJL046W	12	Tricarboxylic-acid pathway (citrate cycle, Krebs cycle, TCA cycle)
YPL252C	6	Homeostasis of metal ions (Na, K, Ca, etc.)
YLR074C	2	tRNA transcription; other control of cellular organization; other transcription activities
YNL123W	7	Osmosensing; protein binding
YGL211W	2	Aminoacyl-tRNA-synthetases; cell wall
YGL211W	2	Assembly of protein complexes; lipid, fatty-acid and isoprenoid biosynthesis; cell wall
YBL055C	7	Oxidation of fatty acids; lipid, fatty-acid and isoprenoid biosynthesis
YDR428C	7	Oxidation of fatty acids; lipid, fatty-acid and isoprenoid biosynthesis
YGR263C	7	Oxidation of fatty acids; lipid, fatty-acid and isoprenoid biosynthesis
YOR093C	7	Oxidation of fatty acids; lipid, fatty-acid and isoprenoid biosynthesis
YGL059W	7	Oxidation of fatty acids; lipid, fatty-acid and isoprenoid biosynthesis
YDR428C	7	Amino acid degradation (catabolism)
YGR263C	7	Amino acid degradation (catabolism)
YOR093C	7	Amino acid degradation (catabolism)
YGL059W	7	Amino acid degradation (catabolism)
YGL059W	7	Osmosensing; protein binding
YJR008W	25	rRNA synthesis
YKL099C	6	rRNA processing
YBL004W	10	rRNA processing
YDL213C	4	rRNA processing
YDR324C	10	rRNA processing
YDR449C	10	rRNA processing
YDR496C	10	rRNA processing
YER082C	10	rRNA processing
YER126C	10	rRNA processing
YFR001W	6	rRNA processing
YGL111W	10	rRNA processing
YGR090W	10	rRNA processing
YGR103W	10	rRNA processing
YGR128C	10	rRNA processing
YGR145W	10	rRNA processing
YHR052W	10	rRNA processing
YHR088W	14	rRNA processing
YHR196W	6	rRNA processing
YHR197W	10	rRNA processing
YJL069C	6	rRNA processing
YJL109C	10	rRNA processing
YKL014C	10	rRNA processing
YKR060W	10	rRNA processing
YKR081C	10	rRNA processing
YLR022C	14	rRNA processing
YLR106C	6	rRNA processing
YLR186W	10	rRNA processing
YLR222C	10	rRNA processing
YLR276C	10	rRNA processing
YLR409C	10	rRNA processing
YMR049C	10	rRNA processing
YMR093W	10	rRNA processing
YNL002C	10	rRNA processing
YNL110C	10	rRNA processing
YNL182C	10	rRNA processing
YNR053C	10	rRNA processing
YOL041C	10	rRNA processing
YOL077C	10	rRNA processing
YOR001W	14	rRNA processing
YOR145C	6	rRNA processing
YPL012W	10	rRNA processing
YPL093W	10	rRNA processing
YPR144C	10	rRNA processing
YDL209C	47	Splicing
YGR278W	47	Splicing
YLR424W	47	Splicing
YPL151C	47	Splicing
YGR156W	16	mRNA processing (splicing, 5', 3'-end processing)

**Table 2.** *Continued*

Protein	<i>P</i> -value (log <sub>10</sub> )	Predicted function
YKL018W	16	mRNA processing (splicing, 5'-, 3'-end processing)
YKL059C	16	mRNA processing (splicing, 5'-, 3'-end processing)
YDR036C	20	Ribosome biogenesis
YDR101C	75	Ribosome biogenesis
YGL129C	20	Ribosome biogenesis
YGR283C	75	Ribosome biogenesis
YIL093C	20	Ribosome biogenesis
YJR014W	75	Ribosome biogenesis
YKL155C	20	Ribosome biogenesis
YMR074C	6	Ribosome biogenesis
YMR158W	75	Ribosome biogenesis
YMR310C	75	Ribosome biogenesis
YNL177C	75	Ribosome biogenesis

The ORF name of proteins is listed in the 'Protein' column, corresponding *P*-value is listed in the middle column and predicted function for each protein is listed in the 'Predicted function' column.

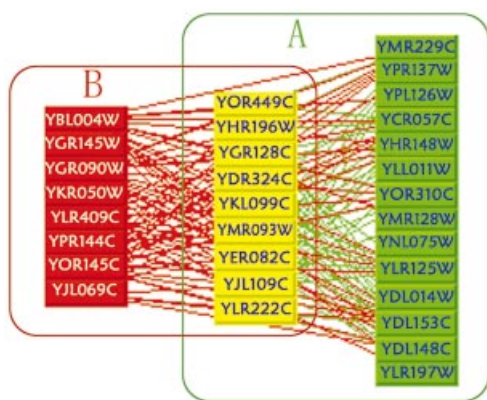


**Figure 3.** Comparison between function prediction and experimental annotation for small subunit (SSU) processome. (A) SSU processome that is supported by experimental evidence (the yellow and the green proteins); (B) our predictions based on quasi-clique 3 (the red proteins and the yellow proteins). The yellow ones are the overlap of (A) and (B). This suggests that our prediction is partly consistent with the experimental evidence (31).

least 50% of proteins, Fig. 2), which imply that those unknown proteins in a same quasi-clique may form a large complex relating to a certain cellular process. For quasi-cliques 3 and 4, most of the proteins were predicted to mediate rRNA processing, which is partly consistent with the results from recent experiments (29,30,31) (Fig. 3).

## DISCUSSION

The yeast large-scale protein–protein interaction data have broadened our view of protein functions in this proteomics era. The biological processes of a cell are controlled by interacting proteins in metabolic and signaling pathways and in complexes such as the molecular machines that synthesize and use adenosine triphosphate, replicate and transcribe genes, or build up the cytoskeletal infrastructure (32,33). The knowledge regarding protein–protein interactions has been accumulated by biochemical and genetic experiments, including

the widely used high-throughput interaction detection methods, such as the yeast two-hybrid system and protein complex purification techniques using mass spectrometry. Now, a challenging task is to decipher the relationships between individual proteins and to understand the molecular organization of cellular networks. Here, for the first time, we analyzed the complicated protein interaction networks using the spectral analysis method. This approach is useful in revealing hidden topological structures, including quasi-cliques and quasi-bipartites, which exhibit meaningful information of a complex network. Figure 4a shows a part of the original interaction network, which contains 109 proteins. It looks confusing and difficult to assimilate before analysis. In contrast, a tightly interacting quasi-clique including 68 proteins was found from this part of network by spectral analysis. This suggests that a network actually is not random as it appears (Fig. 4b).

As part of these studies, we first offered a flexible and promising large-scale protein function prediction system based on spectral analysis. Compared with the previous approaches, what we presented here has a number of practical advantages. Previous methods used partners or neighbors alone to perform the prediction, whereas our method utilized the more informative topological structure of the whole network, and produced some results that were not covered by the previous predictions. The 76 proteins contain 43 rRNA processing proteins, seven proteins related to pre-RNA processing, 11 proteins related to ribosome biogenesis and another 15 proteins related to energy, metabolism, cytoskeleton and transcription regulation. As a control, we created and analyzed random networks with the same interaction distribution as the original network. The results show that among the 48 quasi-cliques of our experimental data, >87.5% were significant in one or more annotation categories at  $P \leq 0.01/N_c$  (here  $N_c$  is the number of categories), whereas <2.1% of quasi-cliques identified from a random network met the same criteria. Some of our predictions have been proved by experiments published recently. This suggests that our prediction method is accurate. Furthermore, this method is a universal one that could be used to predict protein function in other organisms.

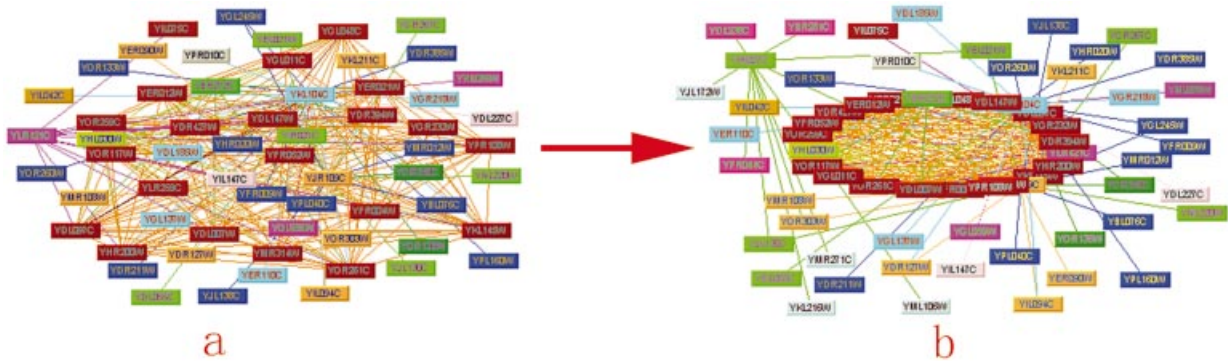


**Figure 4.** Comparison of different visual representations with and without topological structure. The original protein–protein interaction network is rather miscellaneous and difficult to assimilate (a). The spectral analysis revealed a hidden topological structure underlying the miscellaneous network (b).

Although the initial results are promising, the current method is still far from perfect. We have not yet fully explored all quasi-cliques, for that the problem has been proved to be NP-Complete. Therefore new methods should be developed to reveal more sophisticated topological features. It should be pointed out that prediction accuracy is affected by knowledge of known annotations and false positive interactions. It is well known that so far annotations of proteins in databases are incomplete, i.e. a number of proteins with well-characterized function, or at least well-supported functional prediction, are annotated as ‘unknown function’ in MIPS. This introduces additional uncertainties into our prediction. We believe that our prediction would be better if a more accurate interaction and annotation dataset was applied.

## SUPPLEMENTARY MATERIAL

Supplementary Material is available at NAR Online.

## ACKNOWLEDGEMENTS

We would like to acknowledge with deep appreciation Professor Soren Norby for his examining and revising this paper. This work was supported by the Chinese Academy of Sciences Grant No. KSCX2-2-07, National Sciences Foundation of China Grant No. 39890070, the National High Technology Development Program of China under Grant No. 2002AA231031, National Key Basic Research & Development Program (973) under Grant No. 2002CB713805, the National Grand Fundamental Research 973 Program of China under Grant No. G1998030510 and Beijing Science and Technology Commission Grant No. H010210010113.

## REFERENCES

- Fields,S. (1997) The future is function. *Nature Genet.*, **15**, 325–327.
- Rain,J.C., Selig,L., De Reuse,H., Battaglia,V., Reverdy,C., Simon,S., Lenzen,G., Petel,F., Wojcik,J., Schachter,V., Chemama,Y., Labigne,A. and Legrain,P. (2001) The protein–protein interaction map of *Helicobacter pylori*. *Nature*, **409**, 211–215.
- Gavin,A.C., Bosche,M., Krause,R., Grandi,P., Marzioch,M., Bauer,A., Schultz,J., Rick,J.M., Michon,A.M., Cruciat,C.M. *et al.* (2002) Functional organization of the yeast proteome by systematic analysis of protein complexes. *Nature*, **415**, 141–147.
- von Mering,C., Krause,R., Snel,B., Cornell,M., Oliver,S.G., Fields,S. and Bork,P. (2002) Comparative assessment of large-scale data sets of protein–protein interactions. *Nature*, **417**, 399–403.
- Uetz,P., Giot,L., Cagney,G., Mansfield,T.A., Judson,R.S., Narayan,V., Lockshon,D., Srinivasan,M., Pochart,P. *et al.* (2000) A comprehensive analysis of protein–protein interactions in *Saccharomyces cerevisiae*. *Nature*, **403**, 623–627.
- Ito,T., Chiba,T., Ozawa,R., Yoshida,M., Hattori,M. and Sakaki,Y. (2001) A comprehensive two-hybrid analysis to explore the yeast protein interactome. *Proc. Natl Acad. Sci. USA*, **98**, 4569–4574.
- Ho,Y., Gruhler,A., Heilbut,A., Bader,G.D., Moore,L., Adams,S.L., Millar,A., Taylor,P., Bennett,K., Boutilier,K. *et al.* (2002) Systematic identification of protein complexes in *Saccharomyces cerevisiae* by mass spectrometry. *Nature*, **415**, 180–183.
- Cho,R.J., Campbell,M.J., Winzler,E.A., Steinmetz,L. Conway,A., Wodicka,L., Wolfsberg,T.G., Gabrielian,A.E., Landsman,D., Lockhart,D.J. and Davis,R.W. (1998) A genome-wide transcriptional analysis of the mitotic cell cycle. *Mol. Cell*, **2**, 65–73.
- Hughes,T.R., Marton,M.J., Jones,A.R., Roberts,C.J., Stoughton,R., Armour,C.D., Bennett,H.A., Coffey,E., Dai,H., He,Y.D. *et al.* (2000) Functional discovery via a compendium of expression profiles. *Cell*, **102**, 109–126.
- Tong,A.H., Drees,B., Nardelli,G., Bader,G.D., Brannetti,B., Castagnoli,L., Evangelista,M., Ferracuti,S., Nelson,B., Paoluzi,S. *et al.* (2001) Systematic genetic analysis with ordered arrays of yeast deletion mutants. *Science*, **294**, 2364–2368.
- Mewes,H.W., Frishman,D., Gildener,U., Mannhaupt,G., Mayer,K., Mokrejs,M., Morgenstern,B., Munsterkottler,M. *et al.* (2002) MIPS: a database for genomes and protein sequences. *Nucleic Acids Res.*, **30**, 31–34.
- Enright,A.J., Iliopoulos,I., Kyripides,N.C. and Ouzounis,C.A. (1999) Protein interaction maps for complete genomes based on gene fusion events. *Nature*, **402**, 86–90.
- Marcotte,E.M., Pellegrini,M., Ng,H.L., Rice,D.W., Yeates,T.O. and Eisenberg,D. (1999) Detecting protein and protein–protein interactions from genome sequences. *Science*, **285**, 751–753.
- Overbeek,R., Fonstein,M., D’Souza,M., Pusch,G.D. and Maltsev,N. (1999) The use of gene clusters to infer functional coupling. *Proc. Natl Acad. Sci. USA*, **96**, 2896–2901.
- Dandekar,T., Snel,B., Huynen,M. and Bork,P. (1998) Conservation of gene order: a fingerprint of proteins that physically interact. *Trends Biochem. Sci.*, **23**, 324–328.
- Pellegrini,M., Marcotte,E.M., Thompson,M.J., Eisenberg,D. and Yeates,T.O. (1999) Assigning protein functions by comparative genome analysis: protein phylogenetic profiles. *Proc. Natl Acad. Sci. USA*, **96**, 4285–4288.
- Huynen,M.A. and Bork,P. (1998) Measuring genome evolution. *Proc. Natl Acad. Sci. USA*, **95**, 5849–5856.
- Schwikowski,B., Uetz,P. and Fields,S. (2000) A network of protein–protein interactions in yeast. *Nat. Biotechnol.*, **18**, 1257–1261.
- Hishigaki,H., Nakai,K., Ono,T., Tanigami,A. and Takagi,T. (2001) Assessment of prediction accuracy of protein function from protein–protein interaction data. *Yeast*, **18**, 523–531.

20. Maslov, S. and Sneppen, K. (2002) Specificity and stability in topology of protein networks. *Science*, **296**, 910–913.
21. Ge, H., Liu, Z., Church, G.M. and Vidal, M. (2001) Correlation between transcriptome and interactome mapping data from *Saccharomyces cerevisiae*. *Nature Genet.*, **29**, 482–486.
22. Fraser, H.B., Hirsh, A.E., Steinmetz, L.M., Scharfe, C. and Feldman, M.W. (2002) Evolutionary rate in the protein interaction network. *Science*, **296**, 750–752.
23. Gibson, D., Kleinberg, J. and Raghavan, P. (1998) Inferring Web communities from link topology. *Proceedings of the 9th ACM Conference on Hypertext and Hypermedia*. ACM Press, New York, NY.
24. Kleinberg, J. (1998) Authoritative sources in a hyper-linked environment. *Proceedings of the 9th ACM Conference on Hypertext and Hypermedia*. ACM Press, New York, NY.
25. Bollobas, B. (1998) *Modern Graph Theory*. Springer-Verlag, Inc., New York, NY, pp. 3–77.
26. Watts, D.J. and Strogatz, S.H. (1998) Collective dynamics of 'small-world' networks. *Nature*, **393**, 440–442.
27. Tavazoie, S., Hughes, J.D., Campbell, M.J., Cho, R.J. and Church, G.M. (1999) Systematic determination of genetic network architecture. *Nature Genet.*, **22**, 281–285.
28. Wu, L.F., Hughes, T.R., Davierwala, A.P., Robinson, M.D., Stoughton, R. and Altschuler, S.J. (2002) Large-scale prediction of *Saccharomyces cerevisiae* gene function using overlapping transcriptional clusters. *Nature Genet.*, **31**, 255–265.
29. Harnpicharnchai, P., Jakovljevic, J., Horsey, E., Miles, T., Roman, J., Rout, M., Meagher, D., Imai, B., Guo, Y., Brame, C.J. *et al.* (2001) Composition and functional characterization of yeast 66S ribosome assembly intermediates. *Mol. Cell*, **8**, 505–515.
30. Bassler, J., Grandi, P., Gadal, O., Lessmann, T., Petfalski, E., Tollervey, D., Lechner, J. and Hurt, E. (2001) Identification of a 60S preribosomal particle that is closely linked to nuclear export. *Mol. Cell*, **8**, 517–529.
31. Dragon, F., Gallagher, J.E., Compagnone-Post, P.A., Mitchell, B.M., Porwancher, K.A., Wehner, K.A., Wormsley, S., Settlege, R.E., Shabanowitz, J., Osheim, Y. *et al.* (2002) A large nucleolar U3 ribonucleoprotein required for 18S ribosomal RNA biogenesis. *Nature*, **417**, 967–970.
32. Alberts, B., Bray, D., Lewis, J., Raff, M., Roberts, K. and Watson, D.J. (1994) *Molecular Biology of the Cell*, 3rd Edn. Garland, New York, NY.
33. Lodish, H., Berk, A., Zipursky, S.L., Matsudaira, P., Baltimore, D. and Darnell, J. (1995) *Molecular Cell Biology*, 3rd Edn. Scientific American Books, New York, NY.